R02A38B1-0062N BL38B1

X-ray crystallographic analysis of fatty acid β-oxidation multienzyme complex

Momoyo Ishikawa[1] (3750), Daisuke Tsuchiya[1,2] (4400), and *Kosuke Morikawa[1,2] (3651)

1. Biomolecular Engineering Resarch Institute (BERI)
   6-2-3 Furuedai, Suita, Osaka 565-0874
2. Japan Synchrotron Radiation Research Institute (JASRI)
   1-1-1 Kouto, Mikazuki, Sayo, Hyogo

β-oxidation of fatty acid requires a cycle of four sequential reactions, dehydrogenation of an aliphatic hydrogen in acyl-CoA (acyl-CoA dehydrogenase), hydration of the unsaturated aliphatic chain (enoyl-CoA hydratase), dehydrogenation of the hydroxyl group (3-hydroxyacyl-CoA dehydrogenase), and transfer of the acyl group onto free CoA (3-ketoacyl-CoA thiolase). In *Psudomonas fragi*, the last three reactions are catalyzed by a heterotetrameric multienzyme complex, which is composed of two α subunits (73 kDa) and two β subunits (42 kDa). Whereas this subunit composition for fatty acid β-oxidation is found in any organisms, the chain reaction does not always require a similar heterooligomeric structure. This fact may link with a functional merit of multienzymatic complex, which remains unanswered in an atomic level. Three-dimensional structure of the complex is a key to understand the highly coordinated reactions in biological system.

We have succeeded in crystallization of the multienzyme complex (space group: *C*2; a=181 [Å], b=95 [Å], c=161 [Å], and β=111 [°]). To prepare the heavy atom derivative suitable for the structure determination, we substituted cystein residue for Ser40 of the β subunit, which is presumably exposed to solvent region. The mutant protein was crystallized under the presence of methylmercury chloride. The X-ray diffraction images were recorded on ADSC CCD detector at the BL38B1 beamline (λ=1.000 [Å]). The intensity data were indexed and scaled with an R_{merge} of 0.071 upto 3.8 Å resolution. The difference Patterson map with the native data clearly indicated 6 positions of bound Hg atoms. Phasing calculation by multiple isomorphous replacement method is in progress.

R02A38B1-0065N BL38B1

Measurement of the Range and Localization of Secondary Electrons Produced by an X-ray Beam in Gases

Masayo SUZUKI (260) and Hidenori TOYOKAWA (386)

Japan Synchrotron Radiation Research Institute

1. Introduction

The transversal distribution of photoelectrons generated along an X-ray beam in a gaseous medium is mainly determined by (i) the beam size itself (σ_{beam}), (ii) the range of the photoelectrons (R_δ), and (iii) the polarization of the X-ray photons (P). By tracing the trajectories of individual photoelectrons in the medium, one could determine these relevant quantities of R_δ and P, when σ_{beam} is given. Since advanced position-sensitive gaseous detectors are able to reconstruct the trajectories of individual photoelectrons in its detection medium, they could be used for this application, but only when the incident X-ray beam intensity is sufficiently low to the detectors for resolving each event. Certainly they are not applicable to those X-ray beams generated at the 3rd generation synchrotron radiation facilities, the flux of which could reach 10^{15} xph/sec. On the other hand, optical observation of the luminous image induced by an X-ray beam in a heavy rare gas is expected to offer much robust way of determining R_δ and P. It is partially because the luminous image is event-integrated phenomenon, and partially because rare gases are free from radiation damage. The present work reports the preliminary results obtained by observing the luminous image induced in argon gas with X-ray beams of 12 keV and 20 keV.

2. Experimental

A cylindrical vessel made of stainless steel was used as a gas reservoir, which was filled with pure argon gas at 1 atm in the present work. The vessel was equipped with an optical window on its top, through which an image intensifier associated with two microchannel plates was visualizing the luminous images generated in the argon gas. The visualized area in the present work was effectively 170 mm in diameter. The video signals coming from the image intensifier were recorded on a video tape with a conventional video recorder, and were digitized in off-line analysis. The vessel had also an entrance window and an exit window for an incident X-ray beam, which were both made of kapton foil of 50 μm thick. At the BL38B1, the vessel was located on an experimental bench, having the optical window upward. The optical system was aligned such a way that an incident X-ray beam passes in the central region of the visualized images.

Figure 1(a) and (b) display the observed luminous images under irradiation of the X-ray beam with an energy of 12 keV and 20 keV, respectively. In terms of the photoelectron energy ($E_{photoelectron}$), they are corresponding to 8.8 keV and 16.8 keV, respectively. It is clearly seen from these figures that the transversal spread of the visualized image (σ_{ob}) at $E_{photoelectron}$ = 16.8 keV is wider than that at $E_{photoelectron}$ = 8.8 keV. In fact, a simple Gaussian fitting indicates that σ_{ob}(8.8 keV) = 1.5 mm, while σ_{ob}(16.8 keV) = 2.2 mm. Assuming that $\sigma_{ob}^2 = \sigma_{beam}^2 + R_\delta^2$ where σ_{beam} was 2.0 mm in the present work, one could deduce the values of R_δ to be 1.1 mm at $E_{photoelectron}$ = 8.8 keV and 2.0 mm at $E_{photoelectron}$ = 16.8 keV, showing the linear dependence of R_δ on $E_{photoelectron}$.

Fig. 1(a). Luminous image observed with the X-ray beam at 12 keV, corresponding to the photoelectron energy of 8.8 keV. The range of the photoelectrons was estimated to be 1.1 mm.

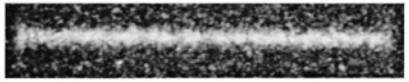

Fig. 1(b). Luminous image observed with the X-ray beam at 20 keV, corresponding to the photoelectron energy of 16.8 keV. The range of the photoelectrons was estimated to be 2.0 mm.